Broadband THz Aqueous Blackbody Calibration Source*

Charles Dietlein[ab], Zoya Popović[a], and Erich Grossman[b]
[a]Dept. of Electrical and Computer Engineering, University of Colorado at Boulder, 425 UCB, Boulder, CO, 80309-0425, USA
[b]Optoelectronics Division, National Institute of Standards and Technology, 325 Broadway, Boulder, CO, 80305-3328, USA

ABSTRACT

We describe a broadband calibration source for the millimeter-wave to terahertz (THz) frequency range, the Aqueous Blackbody Calibration (ABC) source. The blackbody in this design is a body of water, which is extremely absorptive at these frequencies, held by an expanded polystyrene (EPS) holder in a very specific shape, and kept at a uniform known temperature. The undesirable reflectance at the interfaces between the water and the walls of the EPS container is significantly reduced by the use of an "optical trap" geometry. The shape of the custom-molded container is designed so that all radiation incident within the entrance aperture and solid angle of the source undergoes two TE and two TM 45° reflections off the water-EPS interface. This ensures an effective emissivity > 98.5% over the operating band, and has been verified by measurements of EPS transmittance and geometric optics simulation over the entire band. In addition, the effective reflectance of the source is characterized at selected frequencies within the 0.1-2.0THz range.

Keywords: blackbody, calibration, millimeter-wave, terahertz

1. INTRODUCTION

The present activity in millimeter-wave to THz application development[1,2] stimulates a careful examination of measurement accuracies in this spectral band. Accurate measurements of critical figures of merit, such as noise-equivalent power (NEP) and noise-equivalent temperature difference (NETD), are essential in evaluating the suitability of emerging technologies for particular applications. The ABC source was largely developed to answer these concerns for a particular development program concerned with passive millimeter-wave imaging[3]. Its purpose is to emit into free space an absolutely calibrated power spectral density (radiometric temperature) in the spectral region. Combined with an appropriate bandpass filter[4,5,6] it can provide an absolutely calibrated source of power. Among other things, this enables accurate measurement of the responsivity and noise-equivalent temperature difference (NETD) of detector arrays for this spectral band. It is also applicable to ultrawideband spectral measurements, since the radiometric temperature is practically frequency-independent and its frequency dependence is known to a high degree of accuracy. Likewise, when combined with an appropriate mask, it can be used as a scene simulator to generate an accurate spatial profile in radiometric temperature. Blackbody design and absolute radiometry are well developed in the IR and optical bands[7,8], and are key components in providing traceable power measurements in those bands. The ABC source represents an effort to bring similarly systematic and traceable measurement techniques to the millimeter-wave/THz frequency range. Although not intended as a standard reference material, a copy of the core component of the ABC source will be provided by NIST to any party with a legitimate measurement use for it.

A blackbody source must be highly absorptive and its physical temperature must be accurately known. The most common measurement technique for this frequency range uses a millimeter-wave anechoic foam soaked in liquid nitrogen (T = 77 K) as a source. Although such foams are relatively good absorbers, and more sophisticated anechoic materials with even lower reflectance exist[9], the foam rarely remains at 77 K longer than one minute when held in air. Even if left floating in the liquid (which constrains the geometry to vertical beams), its radiometric temperature varies unpredictably. Formation of ice on the foam surface can increase the reflectance in excess of 50%, and moisture increases in the intervening atmosphere and condenses on all exposed surfaces. Heating (rather than cooling) such anechoic materials is an inadequate alternative because they are poor thermal conductors and therefore do not remain isothermal. IR photographs of pyramidal foam panels typically show the tips of the pyramids closer to ambient temperature than the pits between pyramids[10]. On the other hand, a well-mixed and easily heated fluid such as water

Passive Millimeter-Wave Imaging Technology X, edited by Roger Appleby, David A. Wikner,
Proc. of SPIE Vol. 6548, 65480M, (2007) · 0277-786X/07/$18 · doi: 10.1117/12.720165

provides an accurate physical temperature; moreover water is extremely lossy at these frequencies. Unfortunately, the high dielectric constant of water dictates a high reflectance at the water-air interface (R_w), approximately 30% in W-band at normal incidence. This makes the radiometric temperature of a simple water bath highly dependent on the uncontrolled temperature of the ambient surroundings.

2. DESIGN

The basic principle of the ABC source is to combine the isothermal, easily controlled, and convenient aspects of hot water with a geometry that is designed to minimize reflectance from the ambient surroundings. The water must be held in an extremely low-loss container and circulated to remain isothermal. Circulation and heating is achieved by a commercial immersion circulator. The average temperature of the EPS walls, T_e, is the arithmetic mean between the water temperature and the uncontrolled ambient temperature. This is relevant for estimating the uncertainty due to residual absorption in the EPS wall material, which is the dominant uncertainty at high frequency.

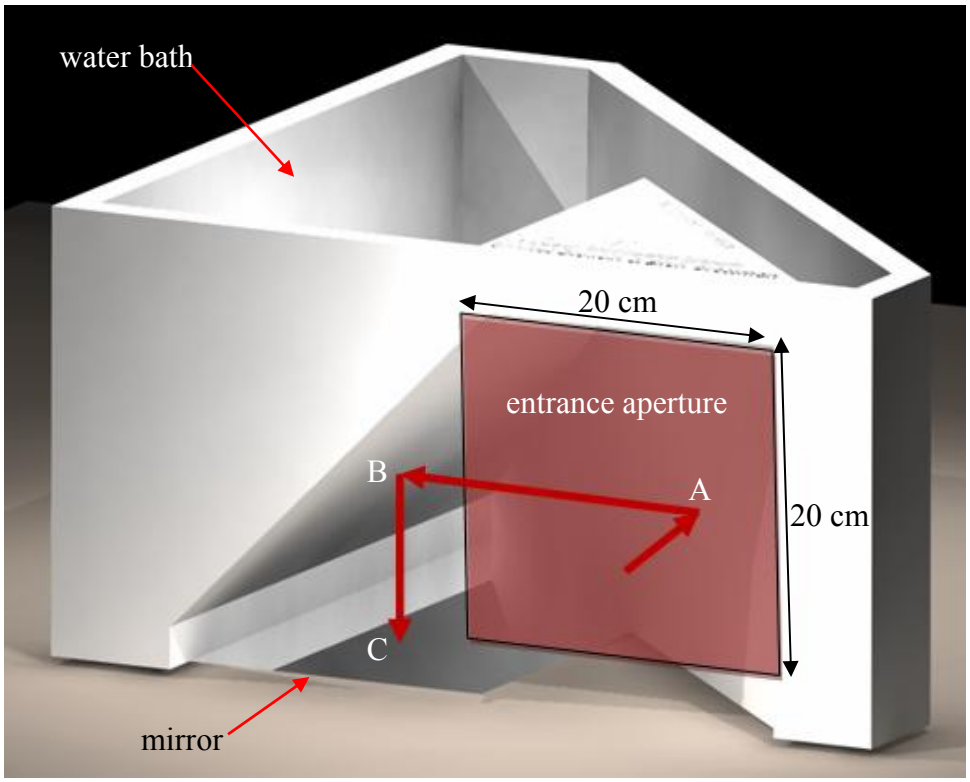

Fig. 1. Trimetric projection rendering of the ABC source. The 20 cm × 20 cm entrance aperture is highlighted. A mirror is placed beneath the second and third water-EPS reflections. Radiation incident on the entrance aperture first encounters a water reflection at surface "A". Reflected radiation is directed to another water reflection at surface "B", then to a mirror surface ("C"), and finally back to water reflections "B" and "A" before exiting the entrance aperture.

Consider the ABC source as an absorber rather than an emitter. Most of the THz radiation incident on the entrance aperture will pass through the container wall and be absorbed in the water behind it (surface "A" in Fig. 1). However, a significant fraction reflects off the interface between the water and the inner surface of the container. The principle underlying the operation of the ABC source is that whatever power reflects off this first water-EPS interface (surface "A") will be directed toward a second EPS wall with water behind it (surface "B"). Similarly, residual power reflected off the second water-EPS interface ("B") is directed onto a third such interface (surface "B" after the mirror reflection "C"), and so on until the residual reflected power is a negligible fraction of the original incident power. All else ideal, $(R_w)^4$ determines the emissivity of the ABC source.

This principle underlies the design of numerous other absorber structures used in absolute radiometry, most notably the "optical trap" detectors developed by Lehman and Cromer[11,12] for absolute calibration of IR photodiode efficiency. The ABC source geometry is essentially a scaled-up version of the four-surface optical trap described by those authors, with the photodiode surfaces replaced by wall-water interfaces. In this geometry, all absorbing surfaces lay at 45° from the normal incident beam. An important point is that the number of TE and TM reflections is equal; this ensures equal reflectance from both horizontally and vertically polarized, as well as any superposition, i.e., unpolarized blackbody radiation.

2.1 ABC source wall material

Because EPS is the lowest-loss solid material known at these frequencies, it has been characterized by a number of authors[13]. Particularly at higher frequencies (f > 500 GHz), its measured properties depend on the manufacturing parameters of the particular sample tested. The most important parameters, given a constant sample thickness, are the density and the bead size of the raw (pre-expansion) material. Before constructing the ABC source, a selection of t = 1 cm thick EPS samples supplied by the same manufacturer, with varying density and bead size, was tested for one-way transmittance with an FTIR. Fig. 2 shows measured transmittance of an ABC source wall from 600 GHz to 6 THz. The selected EPS has an initial average bead diameter d < 0.5 mm with final part density of 55 g/L. The smallest EPS beads commonly available are those with d < 0.5 mm, out of which leak-proof containers (such as coffee cups, with density 96 g/L) are molded. We have found that density is a stronger indicator of transmittance than bead size, as measurements of a 55 g/L, (0.5 mm < d < 0.75 mm) sample yielded remarkably similar results, while measurements with varying density show widely different -3 dB frequencies. The tradeoff encountered as EPS density is decreased is that structural stability is sacrificed; specifically, bowing of the second surface ("B") increases as density decreases. In addition to measurements above 600 GHz, we have also measured transmission at frequencies between 100 GHz and 200 GHz. We found absorption at these frequencies to be less than ±1.5%, limited by the stability of our source.

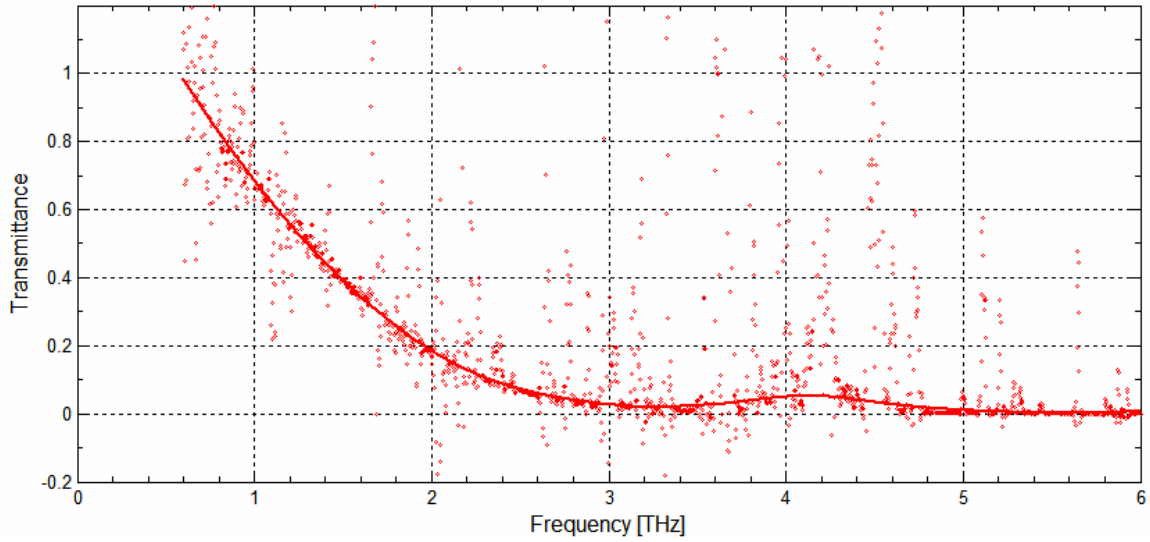

Fig. 2. EPS transmittance at normal incidence, measured with an FTIR, from 600 GHz to 6 THz. The discrepancy around 4 THz is due to a beamsplitter null; transmittance beyond 3.5 THz is zero. Raw data are indicated by points; the thick line shows the data smoothed with a moving average filter.

The ideal perfectly-smooth boundaries between water and EPS are degraded by the surface roughness of the EPS. Although the beads are molded into the desired shape with a smooth mold, small voids between the flattened beads on the surface produce a water surface that is not perfectly flat. After expansion, the beads are measured to be (0.65 mm < d < 0.7 mm), both at the surface and throughout the volume of an ABC source wall. Absorption is not the only loss mechanism encountered, as scattering plays a significant role in EPS transmission[13]. Therefore, in calculating the radiometric temperature T_r at the entrance aperture, the approximation of EPS absorption as $A_e = (1-\tau_e)$ is not a complete description. Absorption is designated A, the subscript e represents EPS, and τ refers to transmission.

2.2 Water

The dielectric constant of liquid water follows a double-Debye model[14] in the millimeter-wave/THz region. Using this model, the Fresnel coefficients are obtained for reflectance at a 45° incidence off an interface between water and EPS, which is assumed to have an index of $n = 1$. The result is shown in Fig. 3. Water reflectance R_w is the limiting factor for the performance of the ABC source at low frequencies ($f < 100$ GHz), given that $(R_w)^4$ is the dominant factor in overall performance. Fig. 3 shows the calculated reflectance from 100 GHz to 1THz at a 45° incidence angle for two linear polarizations and unpolarized radiation.

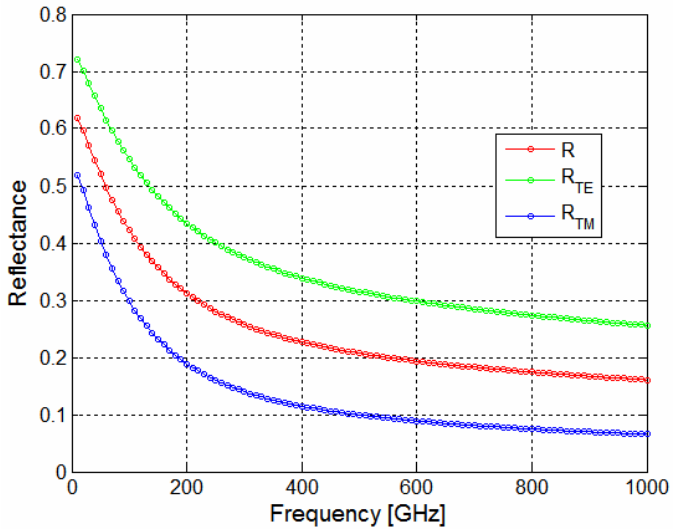

Fig. 3. Reflectance as a function of frequency at a water-air interface, calculated from the double-Debye model[4]. The angle of incidence is 45°. Shown is polarized (TE & TM) and unpolarized radiation. At $f = 100$ GHz, $R_w = 0.41$.

2.3 Geometry

The EPS wall thickness of the two important surfaces in the ABC source is $t = 1.27$ cm; these are the thinnest surfaces in the entire geometry, chosen to bow minimally yet retain high transmittance. Besides the important EPS-water surfaces in the ABC source, the remainder of its geometry is defined by manufacturing constraints. When utilizing small EPS beads, wall thicknesses cannot be greater than 3 cm, or proper fusing of the EPS will not be attained. The sidewalls and the bottom of the ABC source are all 2.5 cm thick, for structural stability and durability. The overall size of the ABC source is 53 cm × 27 cm × 50 cm. When filled with water to completely cover the reflection surfaces, the total water volume is approximately 21 L. To enable the part to release from the two mold halves, the walls are slanted at 1°, such that the sidewalls are slightly wider at the bottom than at the top. To reduce the overall size of the mold, the water area behind the first reflection surface is decreased. When the ABC source is not at a steady-state temperature, i.e. the temperature is being ramped rapidly by the heater, the water temperature T_w behind surface "A" lags the water temperature in the remainder of the ABC source by approximately 90 seconds due to the time constant associated with poor circulation. In steady-state, T_w behind the first surface is the same as T_w throughout the remainder of the volume, within the accuracy of our thermometry (0.2° C).

2.4 Estimated emissivity

Calculating T_r at the entrance aperture requires considering R_w, A_e, the reflectance of the mirror (R_m), as well as accurate knowledge of the temperatures of the water (T_w), the mirror (T_m), the EPS (T_e), and the ambient environment (T_o). The first two parameters are strongly frequency-dependent. Below $f = 100$ GHz, R_w is the limiting factor due to water reflectance exceeding 40% at 45°. At low frequencies, diffraction is also a limiting factor, reducing the effective size of the entrance aperture to maintain acceptably high emissivity. Above $f = 850$ GHz, A_e begins to play a large part in reducing effective emissivity, as $(1-\tau_e)$ increases beyond 20%. The reflectance of the mirror R_m is an overall scale factor, but does not contribute significantly to the final radiometric temperature. Ultimately, with ideal EPS, $(R_w)^4$ dominates the effective emissivity at the entrance aperture.

3. TEST RESULTS

Reflectance at f = 105 GHz was measured by illuminating the entrance aperture of the ABC source with an amplitude-modulated Gunn diode source followed by a scalar feed horn, and raster-mapping the remainder of the entrance aperture with a room-temperature antenna-coupled zero-bias diode[15]. The source was placed in the entrance aperture, off-normal to the entrance aperture, at an angle and offset distance such that the specular reflected beam was located in the center of the other half of the entrance aperture. Therefore, by mapping the half of the entrance aperture not blocked by the source hardware, all of the reflected power is detected. In order to find reflectance as a percentage, raster-mapping of the aperture was performed first with Al mirrors in place of the water on the two reflection surfaces. The mirrors were then removed and the ABC source filled with water, and the aperture mapped again. The summed reflected power detected with the water-filled ABC source is divided by the summed reflected power detected with mirrors as reflecting surfaces, producing a normalized reflectance which can be expressed as a percentage.

Upon analyzing the reflectance maps, it became apparent that the transmitted beam was diverging too rapidly to remain tightly contained in the mapped region. Instead of mapping a bright "spot" in the entrance aperture, the power was spread over the mapped region, falling off at the edges. A PTFE lens was placed after the scalar feed to collimate the source beam. With the lens in place, the entire beam was seen in the mapped region of the entrance aperture, allowing us to confidently state that the effective reflectance is less than 1.5% at f = 105 GHz. A summary of the measured reflectance results is found in Table 1. Due to the weight of the water bowing surface "B", the collimated beam reflected by water was not found at the same location as the collimated beam reflected by the Al mirrors (centered vertically in the aperture), so simple rectangular regions symmetric about the vertical center of the aperture are not valid for calculating normalized reflectance until the peak of the reflected beam is within the rectangle.

Table 1: Reflected power percentages; the sum of reflected power with a water-filled ABC source divided by the sum of reflected power with mirrors placed on the reflecting surfaces. The aperture sizes are vertical heights of the entrance aperture, measured from the vertical center of the ABC source. The width of the aperture area is the full unblocked region of the ABC source.

Aperture size	±2.54 cm	± 3.81 cm	±5.08 cm	±6.35 cm	±7.62 cm	±8.89 cm
105 GHz	0.65%	0.66%	0.68%	0.69%	0.72%	0.75%
105 GHz w/lens	n/a	n/a	n/a	1.41%	1.42%	1.45%

4. DISCUSSION

We have described a new blackbody source for the millimeter-wave to THz frequency regime, with an aperture over 65λ in diameter at f = 100 GHz. The predicted performance when not limited by EPS transmission is given by R_w^4, theoretically providing emissivity over 99% above 200 GHz, where water reflectance at 45° for unpolarized radiation drops below 0.31. The next revision of the ABC source geometry is planned to incorporate smaller dimensions, therefore decreasing the water volume and allowing thinner, lower-density walls. By doing this, EPS transmission will not reduce performance until above 1.5 – 2.0 THz.

Figure 4 shows a passive broadband THz image of the ABC source in an uncontrolled lab environment, overlaid at 50% opacity onto a visible image of the same scene. In the THz image, the obvious hot aperture is visible as a trapezoid. Because the imager was not normal to the ABC source, the deformation of the aperture shape is more obvious. When on-axis and orthographically projected, the aperture remains square. Due to perspective, however, the square becomes a trapezoid when imaged on-axis and normal. From the point of view of the THz imager (Fig. 4), several other warm areas are noted, including a reflection off the optics table in front of the ABC source, the reflecting mirror inside the cavity (surface "C"), and the hot water bath below the immersion circulator. Anechoic material is placed to cover much of the front of the ABC source, to prevent stray radiation from entering the cavity at large angles of incidence.

5. ACKNOWLEDGEMENTS

The authors acknowledge the support of DARPA Microsystems Technology Office and NSF interdisciplinary award #0501578.

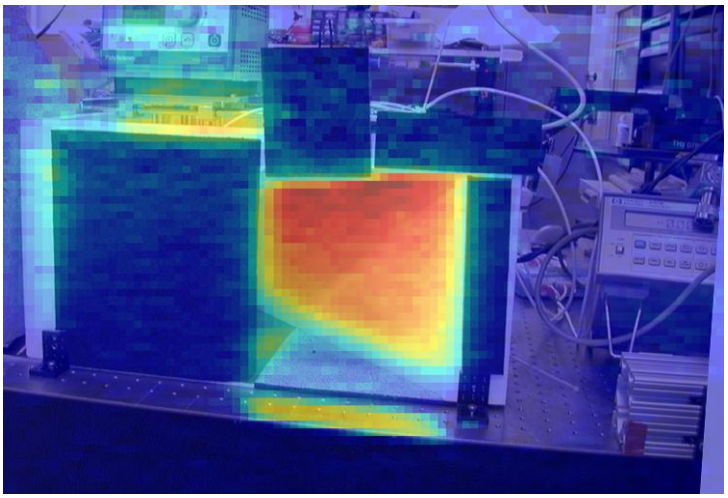

Fig. 4. A visible image of the ABC source from the perspective of the primary aperture of a passive broadband THz imager. Overlaid at 50% opacity is an image taken with the THz imager, showing the trapezoidal aperture of the ABC source, as well as a reflection from the optics table in front of the source, a warm spot on the reflecting mirror (surface "C"), and heat from the water bath beneath the immersion circulator.

REFERENCES

1. D. W. Woolard, Brown, E.R., Pepper, M., and Kemp, M., "Terahertz frequency Sensing and Imaging: A Time of Reckoning Future Applications?" *Proc. of the IEEE*, vol. 93, pp. 1722-1743, 2005.
2. P. H. Siegel, "Terahertz Technology in Biology and Medicine," *IEEE Trans. Microw. Theory Tech.*. vol. 52, pp. 2438-2447, 2004.
3. C. M. Stickley, Filipkowski, M., "Microantenna Arrays: Technology and Applications; MIATA an overview," *Proc. 1st Eurpoean Symposium on Optics and Photonics in Security and Defence*, 2004.
4. E. N. Grossman, Dietlein, C.R.,Luukanen, A.M., "Terahertz Circular Variable Filters," *4th ESA Workshop on Millimetre-wave Technology and Applications*, pp. 353-358, 2006.
5. M. E. MacDonald, A. Alexanian, R. A. York, Z. Popovic, and E. N. Grossman, "Spectral Transmittance of Lossy Printed Resonant-Grid Terahertz Bandpass Filters," *IEEE Trans. Microw. Theory Tech.*, vol. 48, pp. 712-718, 2000.
6. D. W. Poterfield, J.L. Hesler, R. Densing, E.R. Mueller, T.W. Crowe, R.M. Weikle II, "Resonant Metal Mesh Bandpass Filters for the Far-Infrared," *Applied Optics*, vol. 33, pp. 6046, 1994.
7. F. Hengstberger, *Absolute Radiometry*. San Diego, CA: Academic Press, 1989.
8. E. Theocharous, Fox, N.V.,Sapritsky,V.I., Mekhontsev, S.N., and Morozova, S.V., "Absolute Measurements of Black-body Emitted Radiance," *Metrologia*, vol. 35, pp. 549-554, 1998.
9. R. H. Giles, Horgan, T.M., "Method for absorbing radiation." United States Patent no.5,260,513: Univ. of Massachusetts, 1993.
10. A. E. Cox, O'Connell, J.J., and Price, J.P., "Initial results from the infrared calibration and infrared imaging of a microwave calibration target," presented at IEEE Geoscience and Remote Sensing Symposium, Denver, 2006.
11. J. H. Lehman and C. L. Cromer, "Optical trap detector for calibration of optical fiber powermeters: coupling efficiency," *Applied Optics*, vol. 41, no. 31, pp. 6531-6536, Nov. 2002.
12. J. H. Leman and C. L. Cromer, "Optical tunnel-trap detector for radiometric measurements," *Metrologia*, vol. 37, pp. 477-480, 2000.
13. G. Zhao, M. ter Mors, T. Wenckebach, and P. C. M. Planken, "Terahertz dielectric properties of polystyrene foam," *J. Opt. Soc. Am. B*, vol. 19, no. 6, pp. 1476-1479, June 2002.
14. J. T. Kindt and C. A. Schmuttenmaer, "Far-infrared dielectric properties of polar liquids probed by femtosecond terahertz pulse spectroscopy," *J. Phys. Chem.*, vol. 100, pp. 10373-10379, 1996.
15. H. Kazemi, et. al., "Ultra sensitive ErAs/InGaAlAs direct detectors for millimeter wave and THz imaging applications." to be published in IEEE International Microwave Symposium proceedings, 2007.